Classical Nernst engine

Julian Stark,[1] Kay Brandner,[1] Keiji Saito,[2] and Udo Seifert[1]
[1]II. Institut für Theoretische Physik, Universität Stuttgart, 70550 Stuttgart, Germany
[2]Department of Physics, Keio University, 3-14-1 Hiyoshi, Kohoku-ku, Yokohama 223-8522, Japan
(Received 1 October 2013; revised manuscript received 4 March 2014; published 7 April 2014)

We introduce a simple model for an engine based on the Nernst effect. In the presence of a magnetic field, a vertical heat current can drive a horizontal particle current against a chemical potential. For a microscopic model invoking classical particle trajectories subject to the Lorentz force, we prove a universal bound $3-2\sqrt{2}\simeq 0.172$ for the ratio between the maximum efficiency and the Carnot efficiency. This bound, as the slightly lower one $1/6$ for efficiency at maximum power, can indeed be saturated for a large magnetic field and small fugacity.

DOI: 10.1103/PhysRevLett.112.140601 PACS numbers: 05.20.-y, 05.60.Cd, 05.70.Ln, 85.80.-b

Introduction.—The Nernst effect describes the emergence of an electrical voltage perpendicular to a heat current traversing an isotropic conductor in the presence of a constant magnetic field [1]. However, while Seebeck-based devices, for which the heat and the particle current are coupled without a magnetic field, have been the subject of intensive research efforts during the last decades [2–5], only a few attempts were made to utilize the Nernst effect for power generation more than 50 years ago [6–9]. Apparently, our understanding of fundamental aspects of the thermodynamic efficiency of Nernst-based devices has not been updated since then. This lack of interest may have been caused by the uncompetitive net efficiency of such devices, which is inevitably suppressed by the energetic cost of the strong magnetic fields they require. New discoveries in the phenomenological theory of thermoelectric effects as well as recent experiments showing the accessibility of magnetic field effects in nanostructures even at low and moderate field strengths [10–13], however, cast new light on the topic of Nernst engines.

Within the framework of linear irreversible thermodynamics it can be proven, quite generally, that the output power of steady state heat engines vanishes as their efficiency approaches the Carnot value η_C and, moreover, that their efficiency at maximum power is subject to the universal bound $\eta_C/2$ [14]. However, both of these results rely strongly on the time-reversal invariance of the microscopic dynamics, which implies that the off-diagonal Onsager coefficients are identical. In the presence of a magnetic field breaking this symmetry, they must be reassessed. Indeed, by extending the standard analysis, Benenti and co-workers found that thermoelectric efficiency could be increased so significantly by a magnetic field that, in principle, even devices operating reversibly at finite power seem to be achievable [15].

Such an intriguing suggestion asks for a better understanding of coupled heat and particle transport in magnetic fields. First progress in this direction was recently achieved within the paradigmatic class of multiterminal models using the well-established Landauer-Büttiker formalism, within which transport is described as a coherent quantum scattering process of non-interacting particles [16,17]. Inelastic scattering events can be taken into account on a phenomenological level using fictitious terminals, whose temperature and chemical potential are chosen such that they, on average, do not exchange heat or particles with the real terminals [18]. Such probe terminals play a crucial role, since it can be shown that for a pure two-terminal setup the Onsager matrix is always symmetric, even in the presence of a magnetic field [19]. For more terminals, the analysis carried out in [20] and [21] revealed that current conservation implies much stronger bounds on the efficiency than the standard rules of linear irreversible thermodynamics. For the minimal case of three terminals these bounds were even shown to be tight [22]. Since these studies were based on general particle transmission probabilities without reference to any specific microscopic dynamics, they leave the necessary conditions for saturating the new bounds open.

Simple mechanical models have led to remarkable insight into the microscopic mechanisms underlying heat and matter transport [23,24], especially in the context of thermoelectric efficiency [25–27]. So far, the Nernst effect has not yet been addressed using such models. We therefore propose a minimalistic model for such an engine, which relies on a classical formalism inspired by the Landauer-Büttiker approach and provides physical insight on the level of single particle trajectories.

System.—As shown in Fig. 1, we consider a two-dimensional, circular, and potential-free central region of radius R perpendicularly penetrated by a homogeneous magnetic field $\mathbf{B}$ of strength $B\equiv|\mathbf{B}|$, surrounded by four thermochemical reservoirs C_i, each of which covers a segment of length $l\equiv\pi R/2$ of the boundary. The fluxes entering and leaving the system through the reservoirs can be determined as follows. Any particle that reaches the circular boundary from one of the reservoirs is assumed to enter the central region, in which it follows a circular trajectory due to

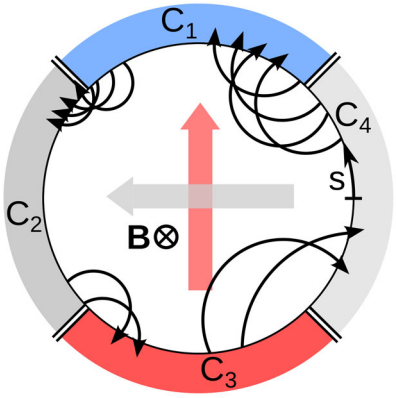

FIG. 1 (color online). Scheme of the classical Nernst engine. The vertical heat current (red arrow) between reservoir C_3 and C_1 with $T_3 > T_1$ drives a horizontal particle current (grey arrow) from reservoir C_4 to C_2 with $\mu_2 > \mu_4$. The circular arrows show typical trajectories for a strong magnetic field $\mathbf{B}$. Their radius and number reflect the temperature and chemical potential, i.e., density, of the respective reservoir they originate from. The coordinate $0 \le s \le 2\pi R$ parametrizes the boundary.

the Lorentz force. Such a minimalistic assumption of perfectly transparent boundaries has been shown to be thermodynamically consistent [28] and allows us to calculate the fluxes explicitly. Maxwell-Boltzmann statistics in the reservoirs modeled as ideal gases maintained at equilibrium with temperature $T_i \equiv 1/\beta_i$ and chemical potential μ_i implies a total particle current [29],

$$J_i^{\varrho+} \equiv \int_l ds \int_0^\infty dE \int_{-\pi/2}^{\pi/2} d\vartheta u_i(E) \cos\vartheta = \frac{\sqrt{2\pi m} l e^{\beta_i \mu_i}}{\beta_i^{3/2} h^2}, \tag{1}$$

flowing from the reservoir C_i into the system, where $u_i(E) \equiv \sqrt{2mE}\exp[-\beta_i(E-\mu_i)]/h^2$, m denotes the mass of the particles, E their kinetic energy, h Planck's constant and Boltzmann's constant has been set equal to 1 throughout this Letter. For the definition of the coordinates s and ϑ, see Figs. 1 and 2. Likewise, assuming that each particle hitting the boundary from inside the central region is

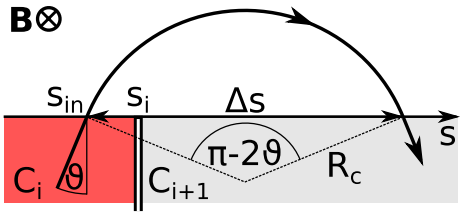

FIG. 2 (color online). Geometry of a single trajectory leaving the reservoir C_i at the position s_{in} with an angle $\vartheta > 0$ and entering the reservoir C_{i+1} at $s_{\text{in}} + \Delta s$. The boundary appears as a straight line, since the Larmor radii are typically small compared to the radius of the central region in the strong field regime. For further symbols, see main text.

absorbed in the adjacent reservoir, the steady-state current flowing into C_i reads

$$J_i^{\varrho-} \equiv \sum_j \int_l ds \int_0^\infty dE \int_{-\pi/2}^{\pi/2} d\vartheta u_j(E) \cos\vartheta \tau_i(E,s,\vartheta). \tag{2}$$

In (2), we have introduced the conditional probability $\tau_i(E,s,\vartheta)$ for a particle of energy E entering at position s with an angle ϑ to reach the boundary of the reservoir C_i after passing through the central region. Since we assume purely Hamiltonian dynamics, this probability can either be 1 or 0. In order to derive a concise expression for the net particle current $J_i^\varrho \equiv J_i^{\varrho+} - J_i^{\varrho-}$ leaving the reservoir C_i, we define the transmission coefficients

$$\mathcal{T}_{ji}(E) \equiv \int_l ds \int_{-\pi/2}^{\pi/2} d\vartheta \tau_j(E,s,\vartheta) \cos\vartheta. \tag{3}$$

As our first main result, we can show that Liouville's theorem implies the sum rules [30]

$$\sum_i \mathcal{T}_{ji}(E) = \sum_j \mathcal{T}_{ji}(E) = 2l. \tag{4}$$

By combining (1), (2), and (4), we finally arrive at

$$J_i^\varrho = \sum_j \int_0^\infty dE \mathcal{T}_{ij}(E)(u_i(E) - u_j(E)). \tag{5}$$

An analogous calculation yields the net heat flux leaving reservoir C_i,

$$J_i^q = \sum_j \int_0^\infty dE \mathcal{T}_{ij}(E)(E-\mu_i)(u_i(E) - u_j(E)). \tag{6}$$

We note that, by virtue of the sum rules (4), the total entropy production $\dot{S} \equiv \sum_i J_i^q / T_i$ accompanying the transport process can be shown to be non-negative [34]. Thus, the relations (4) guarantee the thermodynamic consistency of this formalism.

We now choose the reference values, $\mu \equiv \mu_2$ and $T \equiv T_1$ and define $\Delta\mu_i \equiv \mu_i - \mu$ and $\Delta T_i \equiv T_i - T$. Within the linear response regime, the currents (5) and (6) can be written as

$$J_i^\kappa = \sum_{j\nu} L_{ij}^{\kappa\nu} \mathcal{F}_j^\nu \quad \text{with} \quad \kappa, \nu = \varrho, q, \tag{7}$$

where, we have introduced the affinities $\mathcal{F}_i^\varrho \equiv \Delta\mu_i/T$ and $\mathcal{F}_i^q \equiv \Delta T_i / T^2$, and the Onsager coefficients

$$\begin{pmatrix} L_{ij}^{\varrho\varrho} & L_{ij}^{\varrho q} \\ L_{ij}^{q\varrho} & L_{ij}^{qq} \end{pmatrix} \equiv \int_0^\infty dE u(E) \begin{pmatrix} 1 & E-\mu \\ E-\mu & (E-\mu)^2 \end{pmatrix} \times (2l\delta_{ij} - \mathcal{T}_{ij}(E)) \tag{8}$$

with $u(E) \equiv \sqrt{2mE}\exp[-\beta(E-\mu)]/h^2$.

Operation principle of the Nernst engine.—For a Nernst engine, we put $\Delta\mu_4 < 0$ and $\Delta T_3 > 0$ and impose the boundary conditions

$$J_1^\varrho = J_3^\varrho = 0 \quad \text{and} \quad J_2^q = J_4^q = 0, \tag{9}$$

which allow us to eliminate $\mathcal{F}_1^\varrho, \mathcal{F}_3^\varrho, \mathcal{F}_2^q$ and $\mathcal{F}_4^q$ in (7). These conditions ensure that the particle current occurs only horizontally and heat flows only vertically in the setup of Fig. 1. The operation principle of the Nernst engine can then be understood in terms of typical trajectories as follows. The lower reservoir C_3 is at high temperature but relatively low chemical potential. Therefore, it transmits few but fast particles to the right reservoir C_4. Since this reservoir has lower temperature but higher chemical potential, it injects slower but more particles in order to compensate for the inflowing heat current. Thus, heat is dissipated into the upper, cold reservoir C_1. Now, the number of particles in C_1 has to be conserved on average. Consequently, its chemical potential must be relatively high to ensure that many but slow particles are transferred to the left reservoir C_2. Finally, due to $T_2 > T_1$, a small particle current from C_2 to C_3 is sufficient to compensate for the heat current C_2 has received from C_1. Summing up, the net heat current from C_3 to C_1 drives a particle current uphill from C_4 to C_2.

Bounds on Onsager coefficients and efficiency.—For the current vector $\mathbf{J} \equiv (J_4^\varrho, J_3^q)^t$ and the affinity vector $\mathbf{F} \equiv (\mathcal{F}_4^\varrho, \mathcal{F}_3^q)^t$, we get

$$\mathbf{J} = \mathbb{L}\mathbf{F}, \quad \text{where } \mathbb{L} \equiv \begin{pmatrix} L_{\varrho\varrho} & L_{\varrho q} \\ L_{q\varrho} & L_{qq} \end{pmatrix} \tag{10}$$

is a matrix of effective Onsager coefficients. The two mirror symmetries of our model imply that the off-diagonal entries of this matrix are connected via the relation [34]

$$L_{\varrho q} = -L_{q\varrho}. \tag{11}$$

The output power and efficiency then become $P = -\Delta\mu_4 J_4^\varrho$ and $\eta = P/J_3^q$ [14]. Maximizing η with respect to $\mathcal{F}_4^\varrho$ under the condition $P \geq 0$ yields

$$\eta_{\max} = \eta_C \frac{1-\sqrt{1-\mathcal{Z}T}}{1+\sqrt{1-\mathcal{Z}T}} \quad \text{with} \quad \mathcal{Z}T \equiv \frac{L_{\varrho q}^2}{\det \mathbb{L}}, \tag{12}$$

where $\eta_C \equiv 1 - T_1/T_3 \approx T\mathcal{F}_3^q$ denotes the Carnot efficiency. Obviously, like for conventional thermoelectric devices [15], the maximum efficiency depends only on a single dimensionless quantity, the thermomagnetic figure of merit $\mathcal{Z}T$. This parameter is usually given in the form $\mathcal{Z}T = (NB)^2\sigma T/\kappa$, where NB is the thermomagnetic power, σ the electric and κ the thermal conductivity [1]. However, this definition coincides with the one given in (12), if the transport coefficients NB, σ, κ are identified correctly with the effective Onsager coefficients [35].

Two bounds successively constrain the parameter $\mathcal{Z}T$. First, since the second law requires the rate of entropy production $\dot{S} = \mathbf{F}^t\mathbf{J} = \mathbf{F}^t\mathbb{L}\mathbf{F}$ [37] to be non-negative, the matrix $\mathbb{L}$ must be positive semidefinite. Due to the symmetry (11), this condition reduces to $L_{\varrho\varrho}, L_{qq} \geq 0$. By recalling (12) one has [9]

$$0 \leq \mathcal{Z}T \leq 1. \tag{13}$$

Second, by techniques similar to the ones used in [21], we can show that the Hermitian matrix

$$\mathbb{K} \equiv \mathbb{L} + \mathbb{L}^t + i(\mathbb{L} - \mathbb{L}^t) \tag{14}$$

has to be positive semidefinite as a consequence of the sum rules (4) [30]. This constraint can be expressed as

$$(\det\mathbb{K})/4 = L_{\varrho\varrho}L_{qq} - L_{\varrho q}^2 \geq 0, \tag{15}$$

leading to

$$0 \leq \mathcal{Z}T \leq 1/2. \tag{16}$$

Obviously, the constraint (16), which ultimately relies on Liouville's theorem, is stronger than (13). In particular, while the second law, in principle, allows the maximum efficiency to approach η_C in the limit $\mathcal{Z}T \to 1$, the bound (16) implies the significantly lower limit

$$\eta_{\max} \leq (3 - 2\sqrt{2})\eta_C \simeq 0.172\eta_C. \tag{17}$$

This universal bound on the efficiency of a classical Nernst engine is our second main result. It arises from the four-terminal setup and the symmetry (11) but is independent of further details of the geometry and the strength of the magnetic field. Moreover, (17) would hold for any potential landscape inside the central region preserving the two mirror symmetries of the system. In particular, one may include potential barriers separating the central area from the reservoirs. We note that any additional potential arising from differently biased reservoirs can be safely neglected within the linear response regime, since, quite generally, the linear transport coefficients, i.e., here the Onsager coefficients (10), do not depend on the applied external fields.

Strong field limit.—The existence of a bound provokes the question whether it can be saturated in any given microscopic model. For addressing this issue within our setup, we need to calculate the transmission coefficients $\mathcal{T}_{ij}(E)$ explicitly. To this end, we consider a particle with energy E injected from the reservoir C_i at s_{in} with an angle $-\pi/2 < \vartheta < \pi/2$ as shown in Fig. 2. Due to the Lorentz force, this particle moves on a circle of radius

$$R_c(E) = \sqrt{2mE}c/(|q|B) \equiv \nu(E)R \tag{18}$$

inside the central region and hits the boundary after leaping over a distance Δs measured along the boundary. Here, c denotes the speed of light and $q < 0$ the charge of the particle. We focus on the strong field limit, within which the radii of the Larmor circles $R_c(E)$ are small compared to the radius of the central region, i.e., $\nu(E) \ll 1$, for typical energies E. Consequently, within this regime, the boundary can be treated as a straight line as illustrated in Fig. 2. A simple geometrical analysis then shows

$$\Delta s = 2R\nu(E)\cos\vartheta. \tag{19}$$

Since this quantity is bounded from above by $2R\nu(E) \ll R$, we can consistently assume that particles emitted from the reservoir C_i can either pass to the adjacent reservoir C_{i+1} or return to C_i; i.e., there is transmission of particles only between next neighbor reservoirs. Consequently, we have $\mathcal{T}_{ji}(E) = 0$ for $j \neq i, i+1$. Moreover, the sum rules (4) require $\mathcal{T}_{ii}(E) = 2l - \mathcal{T}_{i+1i}(E)$. Hence, we are left with calculating $\mathcal{T}_{i+1i}(E)$. For this purpose, we recall Fig. 2 and recognize that a particle injected from the reservoir C_i at a certain position s_{in} can reach reservoir C_{i+1} only if $\Delta s \geq s_i - s_{\mathrm{in}}$, where s_i marks the contact point of the reservoirs C_i and C_{i+1}. By virtue of (19), this transmission condition can be rewritten as $\vartheta_- < \vartheta < \vartheta_+$ with $\vartheta_\pm \equiv \pm\arccos[(s_i - s_{\mathrm{in}})/(2R\nu)]$. Finally, by using the definition (3), we arrive at

$$\mathcal{T}_{i+1i}(E) = \int_{s_i-2R\nu(E)}^{s_i} ds_{\mathrm{in}} \int_{\vartheta_-}^{\vartheta_+} d\vartheta \cos\vartheta = \pi R\nu(E). \tag{20}$$

Inserting the transmission coefficients (20) into the general formula (8) for the primary Onsager coefficients and taking into account the auxiliary conditions (9) yields, as our third main result, the effective Onsager matrix

$$\mathbb{L} = \frac{J_0}{2\sqrt{\pi}\mathscr{B}v}\begin{pmatrix} 1 & \sqrt{v-1}/\beta \\ -\sqrt{v-1}/\beta & (1+v)/\beta^2 \end{pmatrix}. \tag{21}$$

Here, we have defined $v \equiv 1 + (2-\beta\mu)^2$ and the dimensionless strength of the magnetic field $\mathscr{B} \equiv |q|BR\sqrt{\beta}/(\sqrt{2m}c)$. $J_0 \equiv (2\pi)^{\frac{3}{2}}\sqrt{m}R\exp[\beta\mu]/(\beta^{\frac{3}{2}}h^2)$ corresponds to the total particle current flowing into the central region at thermal equilibrium, i.e., for $\Delta T_i = \Delta\mu_i = 0$, as one can easily infer from (1). The maximum efficiency in this strong field regime $\mathscr{B} \gg 1$ follows by inserting (21) into (12) as

$$\eta_{\max} = \eta_{\mathrm{C}}\frac{\sqrt{2v}-\sqrt{1+v}}{\sqrt{2v}+\sqrt{1+v}} \quad \text{with} \quad \mathcal{ZT} = \frac{v-1}{2v}. \tag{22}$$

The bounds (16) and (17) are indeed reached for $v \to \infty$, i.e., for $\beta\mu \to -\infty$ [38]. However, in this limit, the equilibrium current $J_0 \sim \exp[\beta\mu]$, and likewise the Onsager matrix (21), decay exponentially. Thus, the saturation of the bounds (16) and (17) comes at the price of vanishing power.

Efficiency at maximum power.—After studying the maximum efficiency of our device, we now consider another important benchmark for the performance of a thermoelectric engine, its efficiency at maximum power η^* [14,39–41], which is obtained by maximizing the output power $P = -\Delta\mu_4 J_4^Q$ with respect to $\Delta\mu_4$. Expressed in terms of $\mathcal{ZT}$, this parameter reads

$$\eta^* \equiv \eta_{\mathrm{CA}}\mathcal{ZT}/(2-\mathcal{ZT}), \tag{23}$$

where $\eta_{\mathrm{CA}} = \eta_{\mathrm{C}}/2$ denotes the Curzon-Ahlborn value [39], which is attained for $\mathcal{ZT} \to 1$. However, the constraint (16) implies the stronger bound

$$\eta^* \leq \eta_{\mathrm{CA}}/3. \tag{24}$$

In the strong field regime, (23) becomes $\eta^* = \eta_{\mathrm{CA}}(v-1)/(3v+1)$. Thus, like $\eta_{\max}$, η^* reaches the bound (24) only in the limit $v \to \infty$, i.e., for $\beta\mu \to -\infty$.

Concluding perspectives.—In this Letter, we have developed a classical formalism to describe heat and particle transport in non-interacting systems, which can be regarded as the classical analogue to the Landauer-Büttiker approach. The crucial quantities of this formalism are the energy-dependent transmission coefficients $\mathcal{T}_{ji}(E)$, for which we have proven the sum rules (4). We emphasize that these sum rules follow solely from Liouville's theorem and thus hold for any kind of Hamiltonian dynamics inside a central region of arbitrary shape.

Using this formalism, we introduced a simple and analytically solvable model for a heat engine based on the Nernst effect, which, mainly for two reasons, is more complex than the Seebeck effect. First, for a sample to be affected by a magnetic field, one needs at least a two-dimensional geometry, allowing the occurrence of looplike trajectories. Second, while in an isotropic Seebeck device heat and particle current are parallel, the Nernst engine requires at least four terminals to allow these currents to run perpendicular to each other.

For the maximum efficiency and the efficiency at maximum power of our engine, we derived universal upper bounds of about 17% of the Carnot value. These bounds can indeed be saturated for a strong field and small fugacities in the reservoirs but only at the price of vanishing power. The analogous results hold for a cooling device based on the Ettingshausen effect [1,34]. In both cases, the bounds would not change even in the presence of an additional potential, for a geometrically deformed central region or for unequal lengths of the boundaries to the respective baths provided the two mirror symmetries are kept [34]. On the one hand, this low value may be regarded as bad news concerning the competitiveness of Nernst based energy converters. On the other hand, they suggest that, from a thermodynamic point of view, Nernst devices are subject to so far unexplored constraints quite different from those applying to Seebeck devices. The question

whether our strong bounds could be lifted in more realistic models including inelastic scattering and particle-particle interactions therefore constitutes an interesting topic for future research. Finally, due to its simplicity and physical transparency, our classical approach can provide a valuable benchmark for assessing the role of quantum effects in future modeling.

U. S. acknowledges support from ESF through the EPSD network. K. S. was supported by MEXT (23740289).

[1] H. J. Goldsmid, *Introduction to Thermoelectricity, Springer Series in Material Science* (Springer, New York, 2009), 1st ed.

[2] M. S. Dresselhaus, G. Chen, M. Y. Tang, R. Yang, H. Lee, D. Wang, Z. Ren, J.-P. Fleurial, and P. Gogna, Adv. Mater. **19**, 1043 (2007).

[3] G. J. Snyder and E. S. Toberer, Nat. Mater. **7**, 105 (2008).

[4] L. E. Bell, Science **321**, 1457 (2008).

[5] C. J. Vineis, A. Shakouri, A. Majumdar, and M. G. Kanatzidis, Adv. Mater. **22**, 3970 (2010).

[6] J. F. Elliott, J. Appl. Phys. **30**, 1774 (1959).

[7] D. A. Wright, Br. J. Appl. Phys. **13**, 583 (1962).

[8] M. H. Norwood, J. Appl. Phys. **34**, 594 (1963).

[9] T. C. Harman and J. M. Honig, J. Appl. Phys. **34**, 189 (1963).

[10] A. G. Pogosov, M. V. Budantsev, D. Uzur, A. Nogaret, A. E. Plotnikov, A. K. Bakarov, and A. I. Toropov, Phys. Rev. B **66**, 201303 (2002).

[11] S. Maximov, M. Gbordzoe, H. Buhmann, L. W. Molenkamp, and D. Reuter, Phys. Rev. B **70**, 121308 (2004).

[12] S. Goswami, C. Siegert, M. Pepper, I. Farrer, D. A. Ritchie, and A. Ghosh, Phys. Rev. B **83**, 073302 (2011).

[13] J. Matthews, F. Battista, D. Sánchez, P. Samuelsson, and H. Linke, arXiv:1306.3694v1.

[14] U. Seifert, Rep. Prog. Phys. **75**, 126001 (2012).

[15] G. Benenti, K. Saito, and G. Casati, Phys. Rev. Lett. **106**, 230602 (2011).

[16] M. Büttiker, Y. Imry, R. Landauer, and S. Pinhas, Phys. Rev. B **31**, 6207 (1985).

[17] M. Büttiker, Phys. Rev. Lett. **57**, 1761 (1986).

[18] M. Büttiker, Phys. Rev. B **33**, 3020 (1986).

[19] M. Büttiker, IBM J. Res. Dev. **32**, 317 (1988).

[20] K. Brandner, K. Saito, and U. Seifert, Phys. Rev. Lett. **110**, 070603 (2013).

[21] K. Brandner and U. Seifert, New J. Phys. **15**, 105003 (2013).

[22] V. Balachandran, G. Benenti, and G. Casati, Phys. Rev. B **87**, 165419 (2013).

[23] C. Mejía-Monasterio, H. Larralde, and F. Leyvraz, Phys. Rev. Lett. **86**, 5417 (2001).

[24] B. Li, G. Casati, and J. Wang, Phys. Rev. E **67**, 021204 (2003).

[25] G. Casati, C. Mejía-Monasterio, and T. Prosen, Phys. Rev. Lett. **101**, 016601 (2008).

[26] M. Horvat, T. Prosen, and G. Casati, Phys. Rev. E **80**, 010102(R) (2009).

[27] K. Saito, G. Benenti, and G. Casati, Chem. Phys. **375**, 508 (2010).

[28] H. Larralde, F. Leyvraz, and C. Mejía-Monasterio, J. Stat. Phys. **113**, 197 (2003).

[29] The mean number of particles with radial momentum in $[p_r, p_r + dp_r]$ and tangential momentum in $[p_s, p_s + dp_s]$, located in a small area $drds$ at the boundary of the reservoir C_i reads $dN_i \equiv \exp[-\beta_i(E-\mu_i)]drdsdp_rdp_s/h^2$. Here, r denotes the radial coordinate and $E = (p_r^2 + p_s^2)/(2m)$ the kinetic energy of the particles. For $p_r < 0$ any particle contributing to dN_i will reach the boundary within the time interval $dt = -mdr/p_r$. Eliminating dr in favor of dt and changing variables due to $p_r \equiv -\sqrt{2mE}\cos\vartheta$, $p_s \equiv \sqrt{2mE}\sin\vartheta$ yields $\dot{N}_i \equiv dN_i/dt = u_i(E)\cos\vartheta dsdEd\vartheta$ with $u_i(E) \equiv \sqrt{2mE}\exp[-\beta_i(E-\mu_i)]/h^2$. Integrating over s, E, ϑ gives expression (1).

[30] See Supplemental Material at http://link.aps.org/supplemental/10.1103/PhysRevLett.112.140601 for technical details, which includes Refs. [31–33].

[31] E. Ott, *Chaos in Dynamical Systems* (Cambridge University Press, Cambridge, England, 2002), 2nd ed.

[32] R. B. Bapat and T. E. S. Raghavan, *Nonnegative Matrices and Applications* (Cambridge University Press, Cambridge, England, 2009), 1st ed.

[33] F. Zhang, *The Schur Complement and its Applications* (Springer, New York, 2005), 1st ed.

[34] K. Brandner, J. Stark, K. Saito, and U. Seifert (to be published).

[35] The standard analysis [36] gives $\sigma = q^2 L_{\varrho\varrho}/T$ and $\kappa = \mathrm{Det}\,\mathbb{L}/(T^2 L_{\varrho\varrho})$, where q is the charge of the particles. The thermomagnetic power is defined as the ratio $NB = V/\Delta T$ of the transverse voltage emerging due to a longitudinal temperature gradient ΔT if the transverse electrical current is held at 0 [1]. Putting $J_4^{\varrho} = 0$ in (10) and solving for $V = -\Delta\mu_4/q$ gives $NB = V/\Delta T_3 = L_{\varrho q}/(TqL_{\varrho\varrho}) < 0$, since $q < 0$.

[36] H. B. Callen, *Thermodynamics and an Introduction to Thermostatics* (Wiley, New York, 1985), 2nd ed.

[37] Since the dynamics inside the central region is purely Hamiltonian, the total rate of entropy production is due to heat dissipated in the four reservoirs, which reads $\dot{S} = -\sum_{i=1}^4 J_i^q/T_i$. Due to the boundary conditions (9), this expression reduces to $\dot{S} = -J_1^q/T_1 - J_3^q/T_3$. By writing, $J_i^q = J_i^E - \mu_i J_i^{\varrho}$, where J_i^E denotes the energy current leaving reservoir C_i, and repeatedly using (9) as well as the conservation laws $\sum_{i=1}^4 J_i^{\varrho} = 0$ and $\sum_{i=1}^4 J_i^E = 0$, we obtain $\dot{S} = ((\mu_2 - \mu_4)/T_1)J_4^{\varrho} + (1/T_1 - 1/T_3)J_3^q$, which, in the linear response regime, becomes $\dot{S} = (\Delta\mu_4/T)J_4^{\varrho} + (\Delta T_3/T^2)J_3^q = \mathbf{F}^t\mathbf{J}$.

[38] The limit $\beta\mu \to +\infty$ is incompatible with our classical approach, since it would lead to an exponentially high equilibrium fugacity $\exp[\beta\mu]$ in the reservoirs [36].

[39] F. L. Curzon and B. Ahlborn, Am. J. Phys. **43**, 22 (1975).

[40] C. Van den Broeck, Phys. Rev. Lett. **95**, 190602 (2005).

[41] M. Esposito, K. Lindenberg, and C. Van den Broeck, Phys. Rev. Lett. **102**, 130602 (2009).